Available online at www.sciencedirect.com

SciVerse ScienceDirect

Journal of the European Ceramic Society 32 (2012) 1893–1899

www.elsevier.com/locate/jeurceramsoc

Sintered silicon nitride/nano-silicon carbide materials based on preceramic polymers and ceramic powder

Ulrich Degenhardt [a], Frank Stegner [c], Christian Liebscher [b], Uwe Glatzel [b], Karl Berroth [c], Walter Krenkel [a], Günter Motz [a,*]

[a] *University of Bayreuth, Ceramic Materials Engineering (CME), D-95440 Bayreuth, Germany*
[b] *University of Bayreuth, Chair of Metals and Alloys, D-95440 Bayreuth, Germany*
[c] *FCT Ingenieurkeramik GmbH, Gewerbepark 11, D-96528 Rauenstein, Germany*

Available online 28 September 2011

Abstract

A flexible method is presented, which enables the fabrication of porous as well as dense Si_3N_4/nano-SiC components by using Si_3N_4 powder and a preceramic polymer (polycarbosilazane) as alternative ceramic forming binder. The SiCN polymer benefits consolidation as well as shaping of the green body and partially fills the interstices between the Si_3N_4 particles. Cross-linking of the precursor at 300 °C increases the mechanical stability of the green bodies and facilitates near net shape machining. At first, pyrolysis leads to porous ceramic bodies. Finally, subsequent gas pressure sintering results in dense Si_3N_4/nano-SiC ceramics. Due to the high ceramic yield of the polycarbosilazane binder, the shrinkage during sintering is significantly reduced from 20 to 15 lin.%. Investigations of the sintered ceramics reveal, that the microstructure of the Si_3N_4 ceramic contains approx. 6 vol.% nano-scaled SiC segregations, which are located both at the grain boundaries and as inclusions in the Si_3N_4 grains.

Keywords: Si_3N_4; Nano-SiC; Precursors-organic; Nanocomposites; Sintering; Microstructure-final

1. Introduction

Silicon nitride ceramics exhibit high mechanical strength and excellent fracture toughness.[1,2] A further improvement of the mechanical properties at room as well as at high temperatures is anticipated on Si_3N_4 materials with nano-scaled SiC segregations.[3–6] These so-called nanocomposite materials, which Niihara et al. developed two decades ago,[3] are fabricated by hot pressing of amorphous SiCN powders. However, the production of the amorphous SiCN powders by processes like the pyrolysis of preceramic polymers,[7,8] CVD,[3,9] SHS[10] or plasma synthesis[11] is difficult and complex.

The processing of Si_3N_4/SiC nanocomposites with beneficial microstructure and properties can be improved by seeding of a conventional Si_3N_4 powder with a smaller amount of amorphous SiCN powders. During sintering of the Si_3N_4, the SiCN separates into nanocrystalline Si_3N_4 and SiC. Typically, the resulting composites consist of elongated, micro-scaled Si_3N_4 grains and up to 10 vol.% nano-scaled SiC segregations, which are located both within the Si_3N_4 host grains and in the grain boundary glassy phase.[4,5] These SiC segregations can act as a reinforcing phase, which increases the bending strength, the fracture toughness and the creep behaviour at high temperatures.[3,5,11,12]

Another way of fabricating Si_3N_4/SiC nanocomposites is the mixing of crystalline Si_3N_4 and SiC nanopowders. However, the homogeneous dispersion of the submicron powders is difficult, and severe agglomeration problems are observed frequently.[12,13] Furthermore, due to the strong crystal growth during sintering, these nanocomposites show a coarser microstructure in comparison to the Si_3N_4/SiC materials seeded with amorphous SiCN.[12,13] These effects usually decrease the mechanical properties of the composites.[12,13]

The main intent of previous investigations on Si_3N_4/SiC composites was to improve the room as well as high temperature properties of the Si_3N_4 ceramic. However, for both the conventional Si_3N_4 and the Si_3N_4/SiC nanocomposite materials, the debinding effort and the high shrinkage during sintering are

* Corresponding author. Tel.: +49 921 555505; fax: +49 921 555502.
E-mail addresses: ulrich.degenhardt@uni-bayreuth.de (U. Degenhardt), f.stegner@fct-keramik.de (F. Stegner), christian.liebscher@uni-bayreuth.de (C. Liebscher), uwe.glatzel@uni-bayreuth.de (U. Glatzel), k.berroth@fct-keramik.de (K. Berroth), walter.krenkel@uni-bayreuth.de (W. Krenkel), guenter.motz@uni-bayreuth.de (G. Motz).

0955-2219/$ – see front matter © 2011 Elsevier Ltd. All rights reserved.
doi:10.1016/j.jeurceramsoc.2011.09.007

Table 1
Elemental composition of the pure polycarbosilazane ABSE and the resulting ceramic material after pyrolysis and gas pressure sintering.

Heat treatment	Empirical formula	Crystalline phases	Free carbon content (mol%)	Ceramic yield (wt.%)	Density (g/cm^3)
Polymer state	$SiNC_2H_6$	–	–	–	1.1
1000 °C/0.1 MPa N_2	$SiN_{0.9}C_{1.5}O_{0.25}H_{0.1}$	–	31	72	2.4
1800 °C/1 MPa N_2	$SiN_{0.08}C_{0.95}O_{0.01}$	β-SiC	–	56	3.2

major problems and make the fabrication extensive and difficult, especially for large ceramic components.

The intention of this work was to develop a processing method, which not only allows the fabrication of Si_3N_4/SiC nano-composites, but also offers the potential to improve the manufacturing of ceramic components in an industrial scale. The combination of a Si_3N_4 powder with a polycarbosilazane instead of an organic binder should be a suitable method to realize these aims. The Si_3N_4 powder particles can be coated homogenously with the preceramic polymer by industrial applicable processes like fluidized bed granulation. In comparison to the use of the amorphous SiCN powders prepared from the precursor an extensive processing like separate pyrolysis, milling, sieving, and mixing with the Si_3N_4 powder is not necessary. Additionally, the alternative ceramic forming binder benefits both the consolidation and shaping, which is also an advantage over the conventional powder technologies for the processing of Si_3N_4 ceramics. Subsequent pyrolysis of the polycarbosilazane binder leads to an amorphous SiCN phase, which partially fills the interstices between the Si_3N_4 particles and reduces the porosity in the resulting porous ceramic bodies.[14,15] During sintering, the homogeneously distributed SiCN phase should lead to the formation of nano-scaled SiC segregations within the Si_3N_4 ceramic. To identify and localize these nano-segregations and to characterize the microstructure as well as the chemical composition of the sintered ceramics comprehensive investigations are necessary. The formation of the SiCN ceramic from the polycarbosilazane binder offers also the potential to reduce the sinter shrinkage of the Si_3N_4 ceramic. Therefore, the influence of the SiCN binder on the shrinkage and the porosity after pyrolysis and gas pressure sintering is studied. Investigations of the green bodies, machinability tests and the manufacturing of prototypes should indicate, whether the Si_3N_4 powder/SiCN precursor method is suitable for the industrial fabrication of complex shaped Si_3N_4 components.

2. Experimental

The polycarbosilazane ABSE (ammonolysed bis(dichloromethylsilyl)ethane) is synthesized in toluene as described elsewhere for silazanes.[16,17] The synthesis yield of the colourless, meltable and soluble precursor is approx. 75 wt.%. Table 1 shows that the ceramization of the precursor at 1000 °C (N_2 atmosphere) results in an amorphous SiCN-ceramic (ceramic yield 72 wt.%). At temperatures above 1400 °C, the SiCN at first crystallizes to the thermodynamically stable phases Si_3N_4, SiC and free carbon.[18] At slightly higher temperatures,[19] the decomposition of the Si_3N_4 and the simultaneous reaction with the free carbon phase according to equation 1 occurs, leading to SiC. After sintering at 1800 °C, mainly crystalline β-SiC has been formed with a ceramic yield of 56 wt.%.

$$Si_3N_4(s) + 3C(s) \rightarrow 3SiC(s) + 2N_2(g) \quad (1)$$

As powder component, Si_3N_4 with a mean particles size (d_{50}) of 650 nm and a specific surface area of 7 m^2/g was used, which already contains 10 wt.% of rare earth and transition metal oxide additives necessary for the liquid phase sintering.

The processing of the ceramic components started with the fabrication of the Si_3N_4 powder/polycarbosilazane precursor mixture by a granulation process described elsewhere.[20,21] The precursor forms an homogeneous coating on the Si_3N_4 powder as well as connects the powder particles with each other. The resulting pourable and non-dusting granulate exhibit a mean granule particle size (d_{50}) of approx. 70 μm and a composition of 80 wt.% Si_3N_4 powder with 20 wt.% polycarbosilazane (42.2 vol.%).

Subsequently, the Si_3N_4/polycarbosilazane granulates were consolidated by uniaxial pressing at 140 MPa to discoidal specimens with 30 mm in diameter and a thickness from 12 to 14 mm. The specimens were thermally crosslinked in a tube furnace at 300 °C (RO 10/100, Heraeus, Hanau, Germany) under continuous nitrogen gas flow (200 cm^3/min). After ceramization of the precursor binder at 1000 °C (N_2 atm.), subsequent liquid phase sintering was accomplished in a gas pressure sinter furnace (FPW 7038, FCT Systeme GmbH, Rauenstein, Germany). To inhibit the thermal decomposition of silicon nitride and to facilitate densification, between 1700 and 1800 °C the nitrogen pressure is raised from 0.2 to 1 MPa.

Dimensional changes and mass losses of the specimens were measured after pyrolysis and gas pressure sintering. From this data, bulk density and shrinkage of the samples were calculated. Specimens powdered with a vibration cup mill (pulverisette 9, Fritzsch GmbH, Idar-Oberstein, Germany) were used for the determination of the skeletal density by Helium pycnometry (Accu Pyc II 1340, Micromeritics Instrument Corp., Norcross, GA, USA). From the difference between the skeletal and the bulk density data, the porosity of the specimens after pressing, pyrolysis and gas pressure sintering was calculated.

The elemental composition of the powdered samples was analyzed at the Pascher Microanalytical Laboratory (Remagen, Germany). The phase composition was investigated with a Philips Xpert X-ray diffractometer (Co anode). Raman spectroscopy measurements were performed with a BX 41 spectrometer (Olympus GmbH, Hamburg, Germany), operating with a HeNe laser (wavelength 632.8 nm) and a beam of 150 μm in diameter.

Table 2
Properties of the Si_3N_4 powder/polycarbosilazane derived materials after pressing, pyrolysis and gas pressure sintering.

Thermal treatment	Uniaxial pressed (RT)	Pyrolyzed (1000 °C)	Gas pressure sintered (1800 °C)
Mass loss (wt.%)	–	5.6	9.1
Skeletal density (g/cm^3)	2.33	2.88	3.23
Bulk density (g/cm^3)	1.98	2.01	3.10
Porosity (%)	14.9	34.0	4.0
Linear shrinkage (lin.%)	–	2.5	16

The sintered Si_3N_4–polycarbosilazane based ceramic was investigated with scanning electron microscopy (SEM, 1540EsB Cross Beam, Carl Zeiss Nano Technology Systems (NTS) GmbH, Oberkochen, Germany) and energy dispersive X-ray analysis (SEM-EDX, Thermo Noran System Six, Thermo Fisher Scientific Inc., Waltham, MA, USA). A lamella of 10 μm × 10 μm and a thickness of approx. 150 nm was prepared within the scanning electron microscope using the focused ion beam (FIB) technique for microstructural characterization in the transmission electron microscope (TEM). The distinction between Si_3N_4 and SiC was performed through a Scanning-TEM (STEM) and a high angle annular dark field (HAADF) detector enabling Z-contrast sensitive imaging (TEM, Libra 200 FE with corrected in-column omega-energy filter, Carl Zeiss NTS GmbH, Oberkochen, Germany), energy dispersive X-ray analysis (TEM-EDS), electron energy loss spectroscopy (TEM-EELS) and energy filtered TEM (EFTEM).

3. Results and discussion

3.1. Pyrolysis and sintering properties

The properties of the Si_3N_4 powder/polycarbosilazane derived specimens after pressing, pyrolysis and gas pressure sintering are listed in Table 2. After pressing, the polycarbosilazane polymer partially fills the pores between the Si_3N_4 powder particles and results in a residual porosity of 14.9%.

The subsequent heat treatment (1000 °C, N_2 atm.) converts the polycarbosilazane binder into an amorphous SiCN ceramic, which remains in the material. Both the density increase and the mass loss of the polycarbosilazane during ceramization (Table 1) cause the shrinkage of the polymer derived ceramic. This behaviour leads also to an increase in porosity of the Si_3N_4/SiCN specimens, whereas the shrinkage of the compact during pyrolysis is only (2.5 lin.%) due to the dimensional stability of the ceramic powder. However, the polymer derived SiCN ceramic is able to bond the Si_3N_4 particles with each other. In contrast to Si_3N_4 components fabricated with conventional acrylic resin binder, the pyrolyzed Si_3N_4/SiCN ceramic offers a remarkable bending strength of approx. 80 MPa after thermal treatment at 1000 °C.[20]

Gas pressure sintering of the porous components leads to nearly dense Si_3N_4 ceramic bodies. The skeletal density of the ceramic specimens increases to 3.2 g/cm^3, which is in accordance with the theoretical density for β-Si_3N_4 and SiC, respectively. During sintering, the shrinkage of the Si_3N_4 powder/polycarbosilazane derived ceramic rises to 16 lin.% with a residual closed porosity of 4%. The reduced shrinkage indicates, that the precursor derived ceramic was partially incorporated in the sintered Si_3N_4 ceramic. However, a mass loss of 3.5 wt.% during sintering denotes further decomposition. To explain the reactions during sintering and to discuss the decomposition behaviour investigations of the chemical composition are required.

3.2. Chemical composition

The measured and the calculated results of the chemical composition of the samples after pressing as well as sintering are summarized in Table 3. The calculations are based on the precursor data (see Table 1) and the fact, that during sintering of the Si_3N_4, usually a mass loss of 2 wt.% due to the evaporation of gaseous SiO occurs.

The measured and the calculated data are in a good agreement for the green bodies. Only the oxygen content is slightly higher than calculated (+1.1 wt.%), whereas the nitrogen concentration in the specimen is lower (−1.3 wt.%). This result can be attributed to the handling and processing of the moisture sensitive polycarbosilazane precursor in air.[22,23]

For the sintered ceramic, the comparison between the measurement and the calculated data shows higher contents of nitrogen and sinter additives than expected, but lower concentrations of the elements Si, O and C than calculated (see Table 3).

Table 3
Elemental composition of Si_3N_4 + 20 wt.% ABSE in the initial state and after gas pressure sintering. Comparison between the calculated and the measured elemental compositions.

Thermal treatment	Data source	Elemental composition (wt.%)					
		Si	N	C	O	H	Sinter additives
Initial state (green body)	Calculated	51.1	31.5	6.7	1.0	1.7	8.0
	Measured	51.1	30.2	6.9	2.1	1.6	8.1
1800 °C/1 MPa N_2	Calculated	56.2	30.2	4.1	1.2	–	8.5
	Measured	54.2	34.3	1.8	0.1	–	9.6

This behaviour can be explained by decomposition reactions, which take place at temperatures above 1400 °C. In contrast to Si_3N_4 ceramics which are fabricated with conventional binders, the polycarbosilazane binder based material contains a high content of fine distributed free carbon even after pyrolysis. This carbon can react not only with the Si_3N_4 (Eq. (1)), but also with the SiO_2, present as an impurity in the polymer derived ceramic as well as in the silicon nitride powder (Eqs. (2) and (3)). As a result the SiO_2 content in the glassy phase during liquid phase sintering is reduced due to the evaporation of gaseous SiO,[4–8] and the carbon content decreases because of the formation of gaseous CO.[24] These gases leave the material or lead to the formation of pores during sintering.

$$SiO_2(s, l) + C(s) \rightarrow SiO(g) + 2CO(g) \quad (2)$$

$$SiO(g) + 2C(s) \rightarrow SiC(s) + CO(g) \quad (3)$$

Beyond the described reactions it has to be considered, that during gas pressure sintering, a nitrogen pressure up to 1 MPa is applied to the ceramic to inhibit the thermal decomposition of silicon nitride and to facilitate the densification. Lenčéš[24] and Kroke et al.[25] described further reactions between the free carbon content, gaseous products like SiO and CO and the nitrogen atmosphere in the furnace. According to the thermodynamic calculations by Kroke et al.[25] the following reactions should be considered under the specific sinter conditions:

$$2SiO(g) + C(s) + N_2(g) \rightarrow Si_2N_2O(s) + CO(g) \quad (4)$$

$$2SiO(g) + 2CO(g) + N_2(g) \rightarrow Si_2N_2O(s) + 2CO_2(g) \quad (5)$$

$$3SiO(g) + 3C(s) + 2N_2(g) \rightarrow Si_3N_4(s) + 3CO(g) \quad (6)$$

In summary, during gas pressure sintering, two types of reactions lead to the consumption of the free carbon content. First, the reactions (Eqs. (2)–(6)) cause formation of volatile CO. This statement is in accordance with the significant loss of carbon, oxygen and silicon (SiO formation, Eq. (2), see also Table 3). Second, due to the reaction of Si_3N_4 (Eq. (1)) and volatile SiO (Eq. (3)) with free carbon, the formation of crystalline SiC is obvious. This result is also reported by van Dijen et al.[26] The authors describe, that during sintering of carbon containing Si_3N_4, the carbon forms crystalline SiC or leaves the material as volatile CO.

For that reason it is of great interest, to bond the carbon as refractory silicon carbide and to distribute the formed SiC particles homogeneously within the sintered Si_3N_4 ceramic.

3.3. Crystalline phases and microstructure

The sintered Si_3N_4/polycarbosilazane based ceramic exhibits a microstructure of elongated Si_3N_4 grains (length up to 8 μm) embedded in grain boundary glassy phase, which is typical for Si_3N_4 ceramics (Fig. 1). Additionally, submicron grains with hexagonal or globular shape are located between the large crystals. However, due to the similar elemental contrast of Si_3N_4 and SiC and the limited resolution of the SEM-EDX system (1 μm in diameter), a distinction between submicron Si_3N_4 and SiC crystals by SEM analysis is not possible.

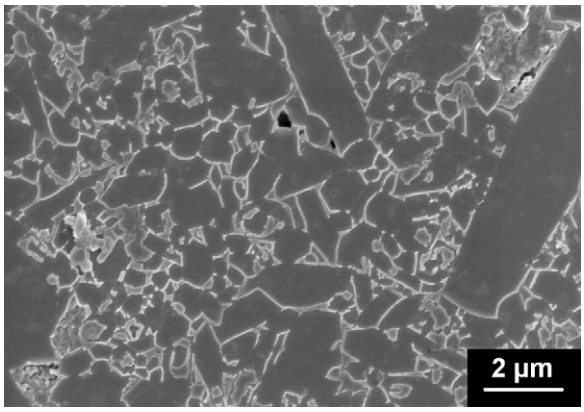

Fig. 1. SEM micrograph of gas pressure sintered Si_3N_4 + 20 wt.% ABSE.

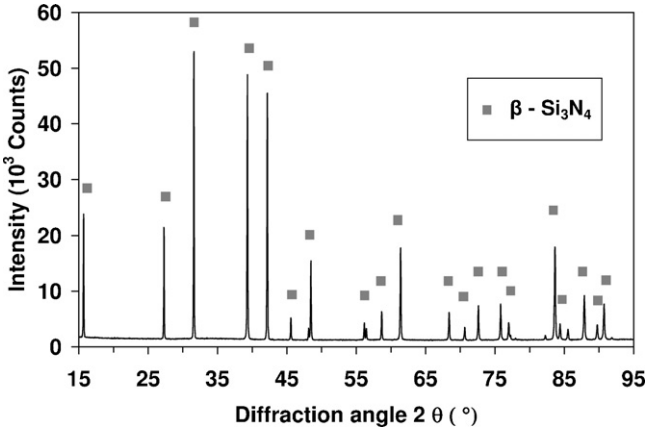

Fig. 2. X-ray analysis of gas pressure sintered Si_3N_4 + 20 wt.% ABSE.

Therefore, the phase composition of the sintered ceramic was investigated with X-ray and Raman spectroscopy. The X-ray spectrum in Fig. 2 shows only signals for crystalline β-Si_3N_4, but no reflexes for the formation of crystalline SiC were detected.

In contrast to the X-ray analysis, Raman spectroscopy measurements indicate the formation of crystalline SiC (Fig. 3). In

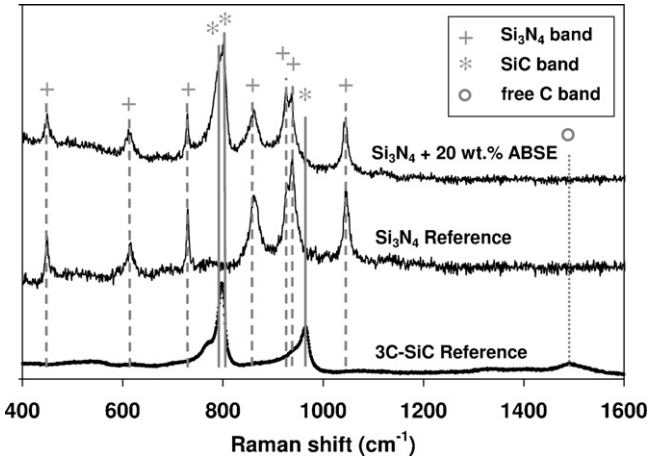

Fig. 3. Raman spectrum of gas pressure sintered Si_3N_4 + 20 wt.% ABSE in comparison to spectra of Si_3N_4 fabricated with conventional acrylic resin binder and polycarbosilane SMP-10 derived SiC (1800 °C, vacuum).

order to identify Si_3N_4, SiC and carbon phases, two reference materials were used. The first reference is a gas pressure sintered Si_3N_4 ceramic fabricated by using a conventional acrylic resin binder. Polymer derived SiC ceramic, synthesized by pyrolysis and crystallization (1800 °C, vacuum) of the polycarbosilane SMP-10 (Starfire Corp., Malta, NY, USA) acts as the second reference.

The spectrum of the Si_3N_4/polycarbosilazane based ceramic shows signals at Raman shifts of 450, 612, 729, 864, 927, 937 and 1045 cm^{-1}, which can be related to crystalline β-Si_3N_4,[27] and two signals for the hexagonal 3C-SiC phase at 798 and 802 cm^{-1}. However, the signal at 966 cm^{-1}, which is also typical for crystalline SiC,[28] could not be detected. This result is in accordance with the results of Zemanova et al.[8] They also report about the missing Raman signal for a sintered SiCN ceramic fabricated from the polysilazane Ceraset (Kion Corp.). In contrast to the SMP-10 derived SiC reference, no signal for free carbon was observed for the sintered precursor/powder based ceramic.

Due to the controversial results of the X-ray and the Raman spectroscopy analysis a detailed TEM investigation should provide for information about the nature of the formed SiC species. Fig. 4 shows submicron crystals within the microstructure of the Si_3N_4/polycarbosilazane based ceramic, which were identified as SiC (marked with green colour) by TEM-EDX investigations. These crystals are located both as segregations embedded in the glassy phase (Inter-SiC) and as randomly distributed inclusions in the elongated Si_3N_4 grains (Intra-SiC). An examination of several TEM images revealed, that the Inter-SiC grains exhibit a median diameter of 50–700 nm, whereas the Intra-SiC inclusions in the Si_3N_4 crystals are much smaller in diameter (20–200 nm).

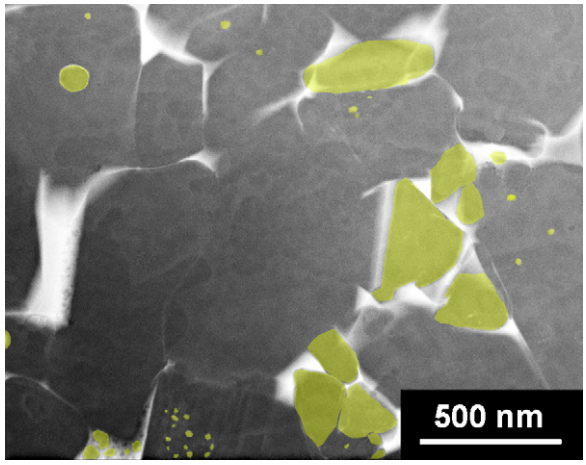

Fig. 4. STEM micrograph of gas pressure sintered Si_3N_4 + 20 wt.% ABSE (Si_3N_4 grains: dark grey, SiC-inclusions: green coloured, grain boundary/glassy phase: white). (For interpretation of the references to colour in this figure legend, the reader is referred to the web version of this article.)

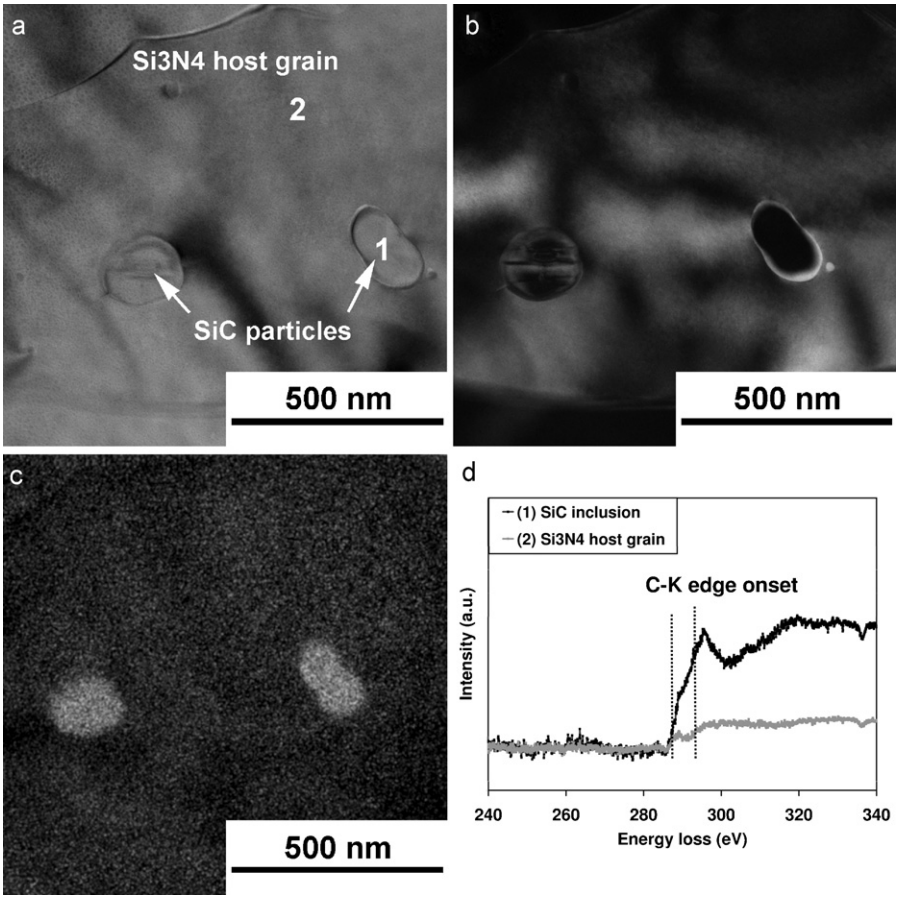

Fig. 5. TEM-EELS-EDX analysis of sintered Si_3N_4 + 20 wt.% ABSE: bright (a) and dark field TEM micrograph (b) of a Si_3N_4 host crystal with nano-SiC inclusions (Intra-SiC) and the corresponding EELS carbon mapping (c) and EELS point measurement spectra (d).

Si_3N_4/SiC nanocomposites with very similar microstructures were also reported by Šajgalík et al.[4,5] and Lenčéš.[24] They used a mixture of conventional Si_3N_4 powder with 10–20 wt.% prepyrolyzed SiCN, which was hot pressed or gas pressure sintered. In good accordance with our results, they obtained Intra-SiC segregations of 10–250 nm embedded in the elongated Si_3N_4 grains and 50–600 nm Inter-SiC crystals in the glassy phase.

The bright and the dark field TEM images in Fig. 5a and b allow for a detailed study of the Intra-SiC inclusions in the Si_3N_4 grains. The corresponding elemental mapping (Fig. 5c) using EFTEM of the C-K edge reveals, that the inclusions (1) contain a higher carbon concentration than the surrounding Si_3N_4 host grain (2). This result is in accordance with the electron energy loss spectra (Fig. 5d) acquired on the particle (1) from Fig. 5a, clearly showing the appearance of the C-K absorption edge with edge onset at an energy loss at 285 eV. In contrast, for the Si_3N_4 host grain, the C-K absorption edge is of considerably lower contrast which is attributed to the thin carbon sputter layer on top of the lamella and the thin carbon film of the TEM-grid.

The TEM investigations clearly indicate that the residual carbon content in the Si_3N_4 ceramic is bonded as crystalline SiC. The reason for the controversial results of the XRD measurement (Fig. 2) is probably the low volume content and the small size of the SiC crystals.

Based on the measured carbon concentration in the sintered specimen (1.8 wt.%, Table 3), the content of crystalline SiC in the Si_3N_4 ceramic can be calculated to 6.0% SiC (both wt.% or vol.%). Compared to the theoretical amount of 13.7% SiC, which was calculated from the theoretical carbon content (4.1 wt.%, Table 3), the loss of carbon during sintering is approx. 65 wt.%. This carbon loss is in accordance with investigations of Riedel et al.[6] They reported, that polycarbosilazane based, sintered SiCN contains only 10% of crystalline SiC instead of the calculated 22%. Similar results were published by Šajgalík et al.[4,5] After gas pressure sintering of 80 wt.% Si_3N_4 with 20 wt.% prepyrolyzed SiCN powder, only 5.5% crystalline SiC segregations were detected.

3.4. Fabrication of prototypes

To investigate the producibility of ceramic components with industrial equipment, thermocouple sheath tube prototypes with 30 mm in diameter and a length of 180 mm were fabricated by cold isostatic pressing (CIP) at 140 MPa by using the polycarbosilazane coated Si_3N_4 powder. After crosslinking at 300 °C, machining tests of green bodies (turning, drilling of holes, cutting in segments) were performed to investigate, whether complex designed components can be realized with the Si_3N_4/polycarbosilazane method. The machined tube segments were pyrolyzed at 1000 °C and subsequent gas pressure sintered at 1800 °C in 1 MPa nitrogen atmosphere.

The sintered thermocouple sheath tube segment in Fig. 6 demonstrates the manufacturing of complex shaped components by the described processing method. In comparison to the standard liquid phase sintered Si_3N_4, for which a conventional acrylic resin binder was used (shrinkage 20 lin.%), the linear

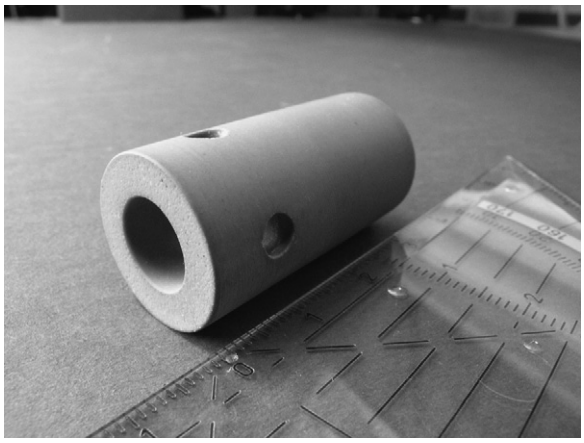

Fig. 6. Cold isostatically pressed, Si_3N_4 + 20 wt.% ABSE derived component after crosslinking, green machining (turning, drilling of holes), ceramization and subsequent gas pressure sintering (1800 °C, 1 MPa N_2 atm).

Table 4
Influence of the binder system on the properties of gas pressure sintered Si_3N_4(/SiC) (compaction: CIP, 140 MPa, gas pressure sintered at 1800 °C, 1 MPa N_2 atm).

Binder system	Acrylic resin	Polycarbosilazane
Original binder content (wt.%)	5	20
Total mass loss (wt.%)	7.0	8.8
Skeletal density (g/cm^3)	3.23	3.23
Bulk density (g/cm^3)	3.20	3.21
Porosity (%)	0.9	0.5
Linear shrinkage (lin.%)	20	15

sinter shrinkage can be reduced to 15 lin.% and the residual porosity to 0.5% (Table 4). The reduced sinter shrinkage can be explained by the high ceramic yield (56 wt.% after sintering, Table 1) of the polycarbosilazane binder, which partially fills up the interstices between the powder particles and reduces the porosity in the preforms (also reported by Schwartz, McGinn et al.[14,15]). During sintering, the precursor derived ceramic is incorporated in the Si_3N_4 and reduces the volume shrinkage of the components. In contrast to the uniaxial pressed green bodies (Section 3.1) with a high residual porosity after pressing (14.9%), the cold isostatic pressing (CIP) improves the compaction of the powder/polycarbosilazane based granulate significantly (porosity after pressing only 10.5%).

The reduced sinter shrinkage offers significant advantages for the fabrication of ceramic components. For example, it allows a reducing of the oversize of the green parts, which is necessary to compensate the volume shrinkage during sintering. Consequently, approx. 20% more components can be placed in the furnace during a sintering cycle. Furthermore, due to smaller tolerances of the sintered components, a reduced hard machining effort can be achieved.

4. Conclusion

Si_3N_4 powder particles were coated homogeneously with a polycarbosilazane by industrial applicable processes like fluidized bed granulation. The resulting granulate was used

for the manufacturing of complex shaped components with industrial equipment. The preceramic polymer acts as an alternative ceramic forming binder, which benefits consolidation and shaping of the ceramic powder. In a first step pyrolysis at 1000 °C leads to porous Si_3N_4/SiCN ceramics. Due to the high ceramic yield, the polymer derived ceramic partially fills the interstices between the Si_3N_4 particles and reduces the porosity in the components. Subsequent gas pressure sintering yielded dense Si_3N_4 ceramics with a nano-scaled SiC content of approx. 6 vol.% derived from the polycarbosilazane. Investigations on the microstructure reveal, that the SiC is located both as segregations in the grain boundaries (Inter-SiC) and as nano-inclusions in the Si_3N_4 grains (Intra-SiC). However, further investigations are necessary to study the influence of the SiC segregations on the mechanical strength, the fracture toughness and the creep behaviour of the silicon nitride ceramic.

The producibility of components was investigated by fabricating thermocouple sheath tube prototypes with industrial equipment. Tooling tests demonstrated the near-net-shape manufacturing of complex shaped components. The ceramic nature of the polycarbosilazane binder after pyrolysis led also to a reduced shrinkage of the components during gas pressure sintering from 20 to 15 lin.%. Therefore, a reduced hard machining effort and saved space in the sinter furnaces can be achieved.

Acknowledgements

The authors gratefully acknowledge the Stiftung Industrieforschung, Cologne, Germany for financial support. We also thank the Clariant Advanced Materials, Sulzbach, Germany for supporting our work and for provide us with preceramic polymers.

References

1. Ziegler G, Heinrich J, Wötting G. Review relationships between processing, microstructure and properties of dense and reaction-bonded silicon nitride. *J Mater Sci* 1987;**22**:3041–86.
2. Riley F. Silicon nitride and related materials. *J Am Ceram Soc* 2000;**83**(2):245–65.
3. Niihara K. New design concept of structural ceramics – ceramic nanocomposites. *J Ceram Soc Jpn* 1991;**99**(10):974–82.
4. Šajgalík P, Hnatko M, Lofaj F, Hvizdos P, Dusza J, Warbichler P, et al. SiC/Si_3N_4 nano/micro-composite – processing RT and HT mechanical properties. *J Eur Ceram Soc* 2000;**20**:453–62.
5. Šajgalík P, Hnatko M, Lenčéš Z. Silicon nitride/silicon carbide nano/micro composites for room as well as high temperature applications. *Key Eng Mater* 2000;**175–176**:289–300.
6. Riedel R, Strecker K, Petzow G. In situ polysilane-derived silicon carbide particulates dispersed in silicon nitride composites. *J Am Ceram Soc* 1989;**72**(11):2071–7.
7. Balog M, Kečkéš J, Schöberl T, Galusek D, Hofer F, Křest'an J, et al. Nano/macro-hardness and fracture resistance of Si_3N_4/SiC composites with up to 13 wt.% of SiC nano-particles. *J Eur Ceram Soc* 2007;**27**:2145–52.
8. Zemanova M, Lecomte E, Šajgalík P, Riedel R. Polysilazane-derived micro/nano Si_3N_4/SiC composites. *J Eur Ceram Soc* 2002;**22**:2963–8.
9. Kavecký Š, Janeková B, Šajgalík P. Composition and morphology control of Si–C–N powders by CVD method. *Key Eng Mater* 2000;**175–176**:49–56.
10. Kata D, Lis J, Pampuch R. Combustion synthesis of multiphase powders in the Si–C–N system. *Solid State Ionics* 1997;**101–103**:65–70.
11. Rendtel A, Hübner H, Herrmann M, Schubert C. Silicon nitride/silicon carbide nanocomposite materials: II. Hot strength creep, and oxidation resistance. *J Am Ceram Soc* 1998;**81**(5):1109–20.
12. Sternitzke M. Review: structural ceramic nanocomposites. *J Eur Ceram Soc* 1997;**17**:1061–82.
13. Niihara K, Hirano T, Nakahara A, Ojima K, Izaki K, Kawakami T. High-temperature performance of Si_3N_4–SiC composites from fine, amorphous Si–C–N powder. *Proceeding of the MRS international meeting on advanced ceramics*, vol. 5. Pittsburgh: Materials Research Society; 1989. p. 107–12.
14. Schwartz KB, Blum Y. Microstructural evidence of interactions in Si_3N_4/polysilazane systems. *Mater Res Soc Symp Proc* 1988;**121**:483–8.
15. McGinn JT, Blum Y, Johnson SM, Gusman MI, McDermott GA. Interactions between crystalline Si_3N_4 and preceramic polymers at high temperature. *Mater Res Soc Symp Proc* 1994;**346**:409–14.
16. Seyferth D, Wiseman GH. High-yield synthesis of Si_3N_4/SiC ceramic materials by pyrolysis of a novel polyorganosilazane. *J Am Ceram Soc* 1984;**67**:C-132.
17. Motz G, Hacker J, Ziegler G. Special modified silazanes for coatings, fibers and CMC's. *Ceram Eng Sci Proc* 2000;**21**:307–14.
18. Traßl S, Motz G, Roessler E, Ziegler G. Characterization of the free-carbon phase in Si–C–N ceramics: I. Spectroscopic methods. *J Am Ceram Soc* 2002;**85**:239–44.
19. Friess M, Bill J, Golczewski J, Zimmermann A, Aldinger F. Crystallization of polymer-derived silicon carbonitride at 1873 K under nitrogen overpressure. *J Am Ceram Soc* 2002;**85**:2587–9.
20. Degenhardt U, Motz G, Krenkel W, Stegner F, Berroth K, Harrer W, et al. Si_3N_4/SiC materials based on preceramic polymers and ceramic powder. *Ceramic Trans* 2010;**209**:379–87.
21. Degenhardt U, Motz G, Krenkel W, Stegner F, Berroth K, Harrer W, et al. Porous Si_3N_4/SiCN materials based on preceramic polymers and ceramic powder. In: Krenkel W, Lamon J, editors. *High temperature ceramic materials and composites*. Berlin: AVISO Verlagsgesellschaft mbH; 2010. p. 675–80.
22. Mucalo MR, Milestone NB, Vickridge IC, Swain MV. Preparation of ceramic coatings from pre-ceramic precursors: Part I. SiC and "Si_3N_4/Si_2N_2O" coatings on alumina substrates. *J Mater Sci* 1994;**29**:4487–99.
23. Günthner M, Kraus T, Dierdorf A, Decker D, Krenkel W, Motz G. Advanced coatings on the basis of Si(C)N precursors for protection of steel against oxidation. *J Eur Ceram Soc* 2009;**29**:2061–8.
24. Lenčéš Z. Factors influencing the crystallization and the densification of ultrafine Si/N/C powders. *Mater Chem Phys* 1995;**41**(1):46–54.
25. Kroke E, Li YL, Konetschny C, Lecomte E, Fasel C, Riedel R. Silazane derived ceramics and related materials. *Mater Sci Eng* 2000;**26**:97–199.
26. van Dijen FK, Kerber A, Vogt U. Special aspects of the sintering of carbothermally synthesized Si_3N_4 powder. *Key Eng Mater* 1994;**89–91**:203–12.
27. Muraki N, Katagiri G, Sergo V, Pezzotti G, Nishida T. Mapping of residual stresses around an indentation in β-Si_3N_4 using Raman spectroscopy. *J Mater Sci* 1997;**32**:5419–23.
28. Nakashima S, Nakatake Y, Ishida Y, Talkahashi T, Okumura H. Detection of defects in SiC crystalline films by Raman scattering. *Physica B* 2001;**308–310**:684–6.